Neural Activity within Area V1 Reflects Unconscious Visual Performance in a Case of Blindsight

Petya D. Radoeva, Sashank Prasad, David H. Brainard, and Geoffrey K. Aguirre

Abstract

■ Although lesions of the striate (V1) cortex disrupt conscious vision, patients can demonstrate surprising residual abilities within their affected visual field, a phenomenon termed blindsight. The relative contribution of spared ''islands'' of functioning striate cortex to residual vision, versus subcortical pathways to extrastriate areas, has implications for the role of early visual areas in visual awareness and performance. Here we describe the behavioral and neural features of residual cortical function in Patient M.C., who sustained a posterior cerebral artery stroke at the age of 15 years. Within her impaired visual field, we found preserved visual abilities characteristic of blindsight, including superior detection of motion, and above-chance discrimination of shape, color, and motion direction. Functional magnetic resonance imaging demonstrated a retinotopically organized representation of M.C.'s blind visual field within the lesioned occipital lobe, specifically within area V1. The incongruity of a well-organized cortex and M.C.'s markedly impaired vision was resolved by measurement of functional responses within her damaged occipital lobe. Attenuated neural contrast-response functions were found to correlate with M.C.'s impaired psychophysical performance. These results demonstrate that the behavioral features of blindsight may arise in the presence of residual striate responses that are spatially organized and sensitive to contrast variation. ■

INTRODUCTION

Although damage to the primary visual cortex (V1) produces contralesional blindness, patients occasionally demonstrate residual visual abilities within the otherwise blind field (Riddoch, 1917). In most such cases, moving stimuli are better detected than stationary (Riddoch, 1917). Further, some patients can also localize targets at above-chance levels within their scotoma through saccades (Poppel, Held, & Frost, 1973), pointing (Weiskrantz, Warrington, Sanders, & Marshall, 1974), or verbal report (Wessinger, Fendrich, & Gazzaniga, 1999), and discriminate target displacements (Blythe, Bromley, Kennard, & Ruddock, 1986), direction of motion (Morland, Le, Carroll, Hoffmann, & Pambakian, 2004), color (Morland et al., 1999), and shape (Wessinger et al., 1999) (for reviews, see Cowey, 2004; Stoerig & Cowey, 1997). The degree of conscious perception in the affected visual field (VF) varies across patients. Some must be induced to ''guess'' to demonstrate their residual capabilities (Tomaiuolo, Ptito, Marzi, Paus, & Ptito, 1997) (a phenomenon also termed Blindsight Type I; Weiskrantz, 1996), whereas others describe vague sensations (Blindsight Type II), although invariably the patients insist that they do not ''see'' within the affected VF (Cowey, 2004; Riddoch, 1917).

University of Pennsylvania

The notion that visual awareness may be dissociated from visual performance has been a provocative one within the philosophy of cognitive neuroscience. Following standard neuropsychological inference, the striking loss of awareness in blindsight has been taken as evidence that the primary visual cortex is the site of conscious visual perception (see Tong, 2003, for a review). This inference is dependent, however, upon the totality of damage to area V1.

Some studies in humans and in animal models support the assertion that visual performance can be mediated by subcortical pathways that bypass the lesioned primary visual cortex and project directly to extrastriate areas (Weiskrantz, 1996; Weiskrantz, Cowey, & Passingham, 1977). Neuroanatomical studies in macaques have demonstrated direct projections from the superior colliculus, and the pulvinar, to the extrastriate cortex (including area MT, the middle temporal area) (Standage & Benevento, 1983). Electrophysiologic studies of macaques with either partial or total ablations of the striate cortex have shown that striate cortex removal did not abolish the visual responsiveness of the majority of MT cells. These residual responses were generally much weaker, although direction selectivity and binocularity were still present (Rodman, Gross, & Albright, 1989). Lesions of both the striate cortex and the superior colliculus abolished these MT visual responses (Rodman, Gross, & Albright, 1990). Combined lesions had similar effects upon the superior

temporal polysensory area (STP) in macaques (Bruce, Desimone, & Gross, 1986). Additionally, multiple studies of hemianopic patient(s) have shown residual visual capabilities after occipital lesions (e.g., for a review, see Stoerig & Cowey, 1997).

Despite this persuasive evidence, a persistent alternative explanation for the phenomenon of blindsight is that small ''islands'' of preserved V1 may mediate spared vision (Scharli, Harman, & Hogben, 1999a, 1999b; Wessinger et al., 1999; Kasten, Wuest, & Sabel, 1998; Wessinger, Fendrich, & Gazzaniga, 1997; Fendrich, Wessinger, & Gazzaniga, 1992). Using an image stabilizer to ensure accurate retinal positioning, Fendrich et al. (1992) performed dense VF mapping in a patient with hemianopia (Patient C.L.T.) (Fendrich et al., 1992). They found an isolated 1° island of residual vision within the affected VF. Stimuli presented to this island could be detected and discriminated above chance, although the patient stated that he ''never saw anything'' despite a sense that ''something happened there'' (Blindsight Type II). Additional psychophysical studies of C.L.T. and other hemianopic patients demonstrated ''islands'' of spared vision in the scotomata of four out of seven patients (Wessinger et al., 1999). Notably, there was considerable variability between and within the subjects. For example, two patients demonstrated localization abilities (F.N. and J.C.) within the islands, two had wavelength discrimination (C.L.T. and J.C.), one had motion detection (F.N.), and one had shape discrimination abilities (C.L.T.) (Wessinger et al., 1999). The authors argued that this variability is not consistent with a subcortical pathway underlying blindsight in these patients, as such a pathway would predict an orderly distribution of abilities throughout the affected VF. Importantly, the anatomical magnetic resonance imaging (MRI) scans of the blindsight patients also revealed remnants of the spared visual cortex within the occipital lesions, which likely mediated the patchy ''island-like'' residual vision.

Several neuroimaging studies have examined visual cortex responses in blindsight. Studies of one patient, G.Y., have demonstrated activation in extrastriate areas, without detectable activation in the primary visual cortex for a range of visual stimuli, including pattern-reversal (Kleiser, Wittsack, Niedeggen, Goebel, & Stoerig, 2001) and moving stimuli (Zeki & Ffytche, 1998), pictures of objects (Goebel, Muckli, Zanella, Singer, & Stoerig, 2001), and emotional faces (producing amygdalar responses; Morris, DeGelder, Weiskrantz, & Dolan, 2001, although see Baseler, Morland, & Wandell, 1999). In a study of seven hemianopic patients, Morland et al. (2004) identified two hemianopes who could discriminate the direction of a drifting grating at above-chance levels (Morland et al., 2004). One of the two patients (Patient G.Y.) showed no activation within the striate cortex, whereas the other patient (R.A.) had calcarine sulcus activation in response to moving and flickering stimuli, consistent with the hypothesis of spared ''islands'' within R.A.'s occipital lesion. It seems that for at least some patients with the neuropsychological phenomenon of blindsight, striate cortex responses to visual stimulation may be observed. The relationship of these residual V1 responses to visual performance, however, remains unclear.

In our current study, we used functional MRI (fMRI) to explore the retinotopic organization and contrast sensitivity of early visual areas of a patient with blindsight (Patient M.C.). We demonstrate that the early visual cortex, including a portion of V1 that appears atrophic on high-resolution MRI scanning, shows preserved retinotopic organization. The visual areas in M.C.'s affected hemisphere also show sensitivity to variations of stimulus contrast, but these responses are attenuated, mirroring M.C.'s psychophysical performance. These results demonstrate that neural responses in V1 can be associated with the behavioral features of blindsight, suggesting that V1 activity does not lead invariably to a perceptual state associated with normal vision.

We should note at the outset that we, along with others (Stoerig & Cowey, 2007; Fendrich, Wessinger, & Gazzaniga, 2001; Scharli et al., 1999a, 1999b; Wessinger et al., 1997, 1999; Kasten et al., 1998; Fendrich et al., 1992), take blindsight to be a description of a behavioral phenomenon, and thus, regard the question of its neural basis as open to experimental investigation. Readers who reserve the term blindsight only for cases where residual visual function exists in the demonstrated absence of functioning V1 may object to our use of the term, but may still find our study of interest in the broader context of the neural basis of residual visual function in cases of perimetric hemianopia.

METHODS

Subject

Patient M.C. suffered a left posterior cerebral artery stroke at the age of 15 years as a consequence of arterial compression from a traumatic occipital subdural collection. Surgical drainage of an additional, left, frontal subdural collection was required. In addition to her visual impairments, she has a mild hemiparesis and dystonia.

Informed consent was obtained and procedures followed institutional guidelines and the Declaration of Helsinki.

Perimetry

Humphrey's automated perimetry was conducted 3 months poststroke using standard clinical equipment (Humphrey Instruments, Field Analyzer Model 750, Serial Number: 7501342). Goldmann's manual perimetry was performed 2 years poststroke (Haag-Streit International, Perimeter 940). The VF is defined by the most peripheral point at

which M.C. was able to detect a stimulus [a disc of 318 cd/m^2 luminance, and an area of 0.25 (I4e) or 64 (V4e) mm^2] moving slowly toward fixation on multiple peripheral-to-central paths.

Behavioral Testing

Detection of the Onsets/Offsets of Moving vs. Stationary Stimuli

The stimuli were moving or stationary 100% contrast square-wave gratings, windowed in a circle with a diameter of 4.2°, centered 19° horizontally from fixation (a 0.3° dot), presented on a background of uniform gray with a luminance equal to the average of that of the gratings. The spatial frequency of all gratings was 0.7 c/deg and temporal frequency for the moving gratings was 4 c/sec. M.C. pressed a button to initiate each trial. This resulted in a change of the color of the fixation point from green to red, which alerted M.C. to the start of the trial. Stimuli appeared after a variable interval (of 2 to 6 sec) and were presented for 3 or 5 sec. M.C. indicated stimulus onset and offset with separate button presses; only the detection of onset performance is reported here. Responses were recorded only if they occurred within 6 sec of the onset or offset of the stimulus. The trials were subject-initiated to allow for resolution of perceptual afterimage. Data were collected in two sessions, separated by a month, 2 years poststroke. Each block of trials lasted for 7 min, and because it was subject-advanced, had a variable number of trials (ranging between 21 and 37). Four blocks (a total of 89 trials) were presented in the affected VF, and three blocks (a total of 109 trials) were presented in the unaffected VF. This study was conducted while M.C. was lying in the scanner and functional scans were acquired, although the fMRI data are not presented here. The remainder of behavioral testing was conducted outside of the scanner.

Detection of Moving Stimuli of Variable Contrast Levels

The stimuli were concentric rings expanding and contracting at 2 c/sec, with a square-wave profile, spatial frequency of 0.6 c/deg, windowed in a circle with a diameter of 8.6°, with the center of the rings 14.7° away from a fixation point (a 0.3° red dot), presented on a background of uniform gray with a luminance equal to the average of that of the rings. Eight different levels of contrast (1%, 3%, 6%, 12%, 25%, 50%, 75%, and 100%) were presented in two types of blocks: higher contrast range (including 6.25%, 12.5%, 25%, 50%, 75%, and 100%), or lower contrast range (1%, 3%, 6%, 12%, 25%, and 100%). The rings were presented on the screen for 2.5 sec. Every 3 sec either a ring or a blank screen appeared, and the central fixation point flickered. The order of presentation of contrast levels was determined by the same pseudorandom sequence used in the fMRI study of contrast sensitivity (see below). M.C. was instructed that whenever the fixation point flickered either a new stimulus would appear, or the screen would be blank. She was to press the spacebar when she detected the presence of a new stimulus. Four testing sessions were conducted over a period of 7 months, 3 to 4 years poststroke. A total of 840 and 404 trials were presented in the affected and in the unaffected VF, respectively.

Direction of Motion Discrimination

Rings of 100% contrast were presented in the same setting as in the Detection of Moving Stimuli experiment (see above). On every trial, the stimulus would either expand or contract within the stimulus window. There were no null trials. M.C. indicated by keypress whether the rings were moving ''in'' or ''out,'' and pressed an additional key to advance to the next stimulus. Three blocks of trials (2 of 48 and 1 of 35 trials) were presented in the affected VF, and two blocks (1 of 48 and 1 of 10 trials) were presented in the unaffected VF. The data were collected 4 years poststroke.

Shape and Color Discrimination

Discrimination of shape and color was performed in separate blocks during one testing session, 4 years poststroke. All stimuli were 9.0° of visual angle and were presented on a white background, with the center of the stimuli 14.7° away from a central fixation point (an ''x''). The stimuli flickered at 10 Hz (50 msec on and 50 msec off) for 800 msec. After the stimuli disappeared from the screen, the central fixation point turned into a ''?'', prompting M.C. to respond. She indicated by keypress the shape or color of the stimulus and pressed an additional key to advance to the next stimulus. A circle, triangle, or square was presented during shape discrimination. These stimuli were black on a white background; as all had the same maximal width/height they did not have equivalent areas. One block of 48 trials was presented in the healthy VF, and two blocks (of 48 trials each) were presented in the affected VF. Red, blue, or green circles (on white background) were presented for color discrimination. These stimuli were not matched in luminance. One block of 48 trials was presented in the healthy VF, and two blocks (one of 82 trials and one of 48 trials) were presented in the affected VF.

Stimulus Presentation

During Behavioral Testing

The shape and color discrimination experiments were programmed in E-Prime (E-Prime, 1.1.4.4) and run on a

PC laptop (Dell, Latitude, D600). The other behavioral experiments were programmed in Matlab and run on a Macintosh laptop (PowerBook G4, model number A1025, with operating system Mac OS 9.2.2). All stimuli were displayed on a CRT monitor (Trinitron, Multiscan 210GS, Sony), at a viewing distance of approximately 59 cm. A chin rest was used to stabilize M.C.'s head position. For experiments where contrast was varied, the spectral power distributions of the monitor's phosphors, as well as the nonlinear input–output relations, were characterized using a PhotoResearch PR-650 spectral radiometer, and these data were incorporated into calculations of the digital RGB values required to produce stimuli of desired contrasts. During pilot testing sessions, eye movements were monitored with a Red-II infrared camera and iView 3.01.23 analysis software (SensoMotoric Instruments). In over 200 trials with monitored eye movements, there were no trials in which M.C. made significant excursions (>2°). Eye-tracking data were not collected for subsequent behavioral experiments.

During MRI Scanning

The visual stimuli were projected (Epson 8100 LCD projector equipped with a Buhl long-throw lens) onto a mylar screen at the rear of the magnet. The subject viewed the stimulus through a mirror mounted on the head coil (the field of view was 22° horizontal × 17° vertical). The video signals were transmitted to the projector using an optical fiber interface (Lightwave Communications, PC FiberLynx Transmitter). The spectral power distributions of the three channels of the projector, as well as the nonlinear input–output relation (gamma functions) for each channel, were characterized in situ using a PhotoResearch PR-650 spectral radiometer. The measured input–output relations were incorporated into calculations of the digital RGB values required to produce stimuli of desired contrasts. Contrast values specified for these experiments are nominal, as actual contrasts deviated slightly from the nominal values due to quantization in the digital-to-analog and analog-to-digital conversions performed by the computer's graphics board, the FiberLynx interface, and the LCD projector itself.

MR Scanning Protocol

Structural and functional data were collected on a 3.0-Tesla Siemens Trio scanner using either an eight-channel head coil or a standard quadrature coil. High-resolution T1-weighted structural images were collected in 160 axial slices and near-isotropic voxels (0.9766 mm × 0.9766 mm × 1.0000 mm; TR = 1620 msec, TE = 3 msec, TI = 950 msec). An additional series of T2-weighted coronal images through the occipital lobe were acquired with 0.4 mm in-plane and 2 mm through-plane resolution for better visualization of the lesioned cortex. Functional blood oxygenation level-dependent (BOLD) echo-planar data were acquired in 3 mm isotropic voxels (TR = 3000, TE = 30). BOLD data were acquired in 42 axial slices (for the retinotopic mapping scans and 4 of the contrast sensitivity scans) or in 30 coronal slices covering the posterior portion of the brain (for the remaining contrast sensitivity scans), and in an interleaved fashion with 64 × 64 in-plane resolution. The first 6 sec of each scan consisted of ''dummy'' gradient and radio-frequency pulses to allow for steady-state magnetization during which no stimuli were presented and no fMRI data were collected.

Neuroimaging Stimuli and Task

In both studies, M.C. monitored a fixation point and was asked to press a key whenever the dot flickered. This was done to ensure accurate fixation.

Standard retinotopic mapping stimuli were used (Engel, Glover, & Wandell, 1997) to map the eccentricity and polar angle representation, and to determine the borders between visual areas. An expanding ring (2 Hz flickering, black-and-white checkerboard presented on a gray background) was used to map the eccentricity representation. M.C. fixated on a red dot, presented 0.04° from the left or right of the edge of the screen, while the ring expanded into the periphery of the left or the right hemifield, in 16 eccentricity steps, each lasting 3 sec (one TR). The ring width varied exponentially with eccentricity and ranged from 0.6° to 6.7° of visual angle. The annulus completed 10 cycles of expansion during each scan (scan time = 10 × 48 sec = 8 min). A rotating 22.5° wedge (also 2 Hz flickering checkerboard) was used to map the polar angle. The wedge stimulus rotated clockwise and traversed one hemifield in 48 sec (16 steps of 3 sec/1 TR).

Retinotopic mapping data were acquired during eight scanning sessions over a period of 3 months. Each scanning session consisted of two to four 8-minute-long scans (160 TRs), and an anatomical MP-RAGE scan. Eight scans (4 right VF [RVF] and 4 left VF [LVF] scans) were excluded because of visible motion artifacts that were present even after the standard motion correction procedures had been applied. A total of 16 scans were included in the final analysis (2 for LVF eccentricity, 7 for RVF eccentricity, 3 for LVF polar angle, and 4 for RVF polar angle). More data were acquired for the affected VF (RVF) to increase our sensitivity for signal from the affected left hemisphere. Additionally, the LVF and the RVF were studied in separates scans to (1) maximize the visual angle of stimulation within each VF and (2) avoid head and eye motion induced by shifts of the fixation point during each scan.

To measure neural contrast sensitivity, stimuli and timing parameters similar to those of the Detection of Moving Stimuli experiment (see above) were used, although there were several differences. Namely, the

stimulus had a diameter of 8.5°, with the center of the rings 13.8° away from the fixation point (a 0.3° red dot). Additionally, M.C. was asked to detect the flickering of the central fixation point (rather than the appearance of a new stimulus in the periphery). The data were acquired during nine scanning sessions over a period of 7 months. Each scanning session consisted of two to four scans of 168 TRs, and an anatomical MP-RAGE scan. Eleven scans (5 RVF and 6 LVF scans) were excluded due to visible motion artifacts that were present even after the standard motion correction procedures had been applied. A total of 19 scans were included in the final analysis (7 for LVF and 12 for RVF). The order of stimulus presentation was determined using the Optseq2 routine (http://surfer.nmr.mgh.harvard.edu/optseq/).

M.C. showed good accuracy rates for the fixation vigilance task. For the scans included in the analysis, she detected 96.1 ± 2.6% [*SD*] of the flickers during the retinotopy scans (95 ± 2.6% for RVF scans and 98 ± 0.8% for LVF scans), and 74 ± 15.6% during the contrast sensitivity scans (76 ± 16% for RVF scans and 71 ± 16% for LVF scans). A more challenging central fixation task was used during most of the contrast sensitivity scans (27 of 30 scans), in which the flicker was smaller and briefer, accounting for the lower performance accuracy. Brain volumes acquired during periods when M.C. failed to detect the flicker were excluded from the contrast-response analysis.

Image Preprocessing

Off-line data analysis was performed using VoxBo (www.voxbo.org) and SPM2 (www.fil.ion.ucl.ac.uk/) software. Data were sinc interpolated in time to correct for the slice acquisition sequence, motion corrected with a six-parameter, least squares, rigid-body realignment routine using the first functional image as a reference, coregistered to the anatomical image, and then normalized in SPM2 to a standard template in Montreal Neurological Institute (MNI) space. Normalization maintained 3 mm isotropic voxels and used 4th degree B-spline interpolation. The fMRI data were smoothed in space with a 0.3-voxel full-width half-maximum isotropic Gaussian kernel. For each dataset, the average power spectrum across voxels and across scans was obtained, and the (square root) of the power spectrum fit with a 1/frequency function (Zarahn, Aguirre, & D'Esposito, 1997). This model of intrinsic noise was used during regression analyses with the Modified General Linear Model (Worsley & Friston, 1995) to inform the estimation of intrinsic temporal autocorrelation.

Anatomical data from the subject were processed using the FMRIB Software Library (FSL) toolkit (www.fmrib.ox.ac.uk/fsl/) to correct for spatial inhomogeneity and to perform nonlinear noise reduction. The average of four separate MP-RAGE images was used to create a high-precision anatomical image. The borders of the lesioned cortex were defined on this averaged MP-RAGE scan by a neurologist not affiliated with this study. The anatomical image was also processed within the BrainVoyager package (BrainInnovation; www.brainvoyager.de/) to identify the gray–white cortical boundary and produce flattened cortical surfaces for data presentation.

Image Statistical Analysis

Statistical analysis of the data was conducted within the modified general linear model (Worsley & Friston, 1995). For the retinotopic mapping data, covariates of interest were modeled as sines and cosines at the fundamental and harmonic frequencies of the task. For the contrast-response dataset, covariates of interest were created as delta functions modeling the different contrast levels, convolved with a standard hemodynamic response function (Aguirre, Zarahn, & D'Esposito, 1998). Covariates of no interest included global signals, scan session, and spikes. The last of these were modeled as impulses, aligned with large transients in the data identified by automated analysis and visual inspection, thought to represent head motion.

The areas of retinotopic response were identified using an F test applied to the conjoint explanatory power of the sine and cosine covariates at the fundamental task frequency, and thresholded at $F > 2$, with at least 5 contiguous voxels. These maps were created separately for the eccentricity and polar angle data, and any voxels present in both maps (the intersection) identified for further analysis. Only regions of response greater than 100 voxels in size were retained for the combined map. Eccentricity and polar angle phase values were calculated for each voxel by taking the arc tangent of the ratio of the sine and cosine component.

The statistical results from the contrast-response fMRI data were evaluated using the comparison of the 100% contrast condition with the null trials. The resulting map was thresholded at t of 3 with a cluster requirement of greater than 3 voxels, with 1019 effective degrees of freedom for the affected VF and 489 effective degrees of freedom for the unaffected VF. Mapwise significance was evaluated using random field theory (Worsley et al., 1996), as extended for cluster thresholding (Cao, 1999). Intrinsic map smoothness was estimated from the model residuals (Kiebel, Poline, Friston, Holmes, & Worsley, 1999). Evaluated within the region of interest defined by the retinotopic mapping protocol for each hemisphere (~1800 voxels), our threshold corresponds to a mapwise alpha <.03 for clusters of 4 or more voxels (calculated with stat_threshold; www.math.mcgill.ca/keith/fmristat). The neural contrast-response function plots were first obtained from the lesioned hemisphere within the clusters of active voxels identified at this threshold. Within the healthy hemisphere, the equivalent number of voxels with the highest statistical value

was identified in each corresponding visual area. The data points on the resulting plots were fit with a Naka–Rushton function (Naka & Rushton, 1966).

RESULTS

Patient M.C. has Residual Visual Function Characteristic of Blindsight

Patient M.C. sustained a left posterior cerebral artery stroke in 2002 at the age of 15. Structural MRI scans identify a lesion within the mesial occipital lobe extending 3.5 cm dorsal and 1 cm ventral to the calcarine sulcus. Recent MRI studies demonstrate atrophy and gliosis in the area of the lesion, with concomitant ex vacuo enlargement of the ventricles (Figure 1A). The stroke caused a right homonymous hemianopia as demonstrated by Humphrey automated visual perimetry (Figure 1B). Subsequent manual Goldmann perimetry demonstrated a hemianopia with approximately 5° of macular sparing (Figure 1B). In the months following her stroke, M.C. noted a vague perception of motion in the affected VF. These sensations were perceptually altered, and appeared slowed and delayed (palinopsia), often with a superimposed, colorful afterimage.

We conducted a series of behavioral tests to characterize M.C.'s perceptual abilities within the impaired field. For these tests, stimuli were presented between 10° and 21° eccentricity while M.C. maintained central fixation. Initial studies conducted 2 years after her stroke demonstrated superior detection of moving stimuli (95%) as compared to stationary stimuli (51%) within her blind field (Figure 1C). Detection of stimuli within her intact field ranged between 96% and 98%. Response times to moving stimuli were also substantially delayed within the blind field compared to the intact field (reaction times ± *SD*: 1.21 ± 1.12 sec vs. 0.36 ± 0.15).

More recently, we have tested M.C.'s ability to discriminate the direction of motion of expanding and contracting rings, and the shapes or colors of flickering stimuli presented in the affected VF. Although M.C. is aware that a moving/flickering stimulus is presented, she reports that she is only "guessing" regarding the property to be discriminated. Nonetheless, her performance was above chance in the impaired VF for shape (60%, binomial distribution $p < .0001$), color (63%, $p < .0001$), and motion direction (60%, $p < .01$) (Figure 1D). M.C.'s discrimination performance was perfect in the intact VF. We note that luminance confounds were present in our tests of color and shape discrimination that could have influenced her performance.

The Damaged Hemisphere Contains Retinotopically Organized Visual Cortex

We next asked if M.C.'s spared perception is associated with functional cortex within early visual areas, including the primary visual cortex (V1). Using retinotopic mapping techniques (Engel et al., 1994; Sereno, McDonald, & Allman, 1994), we measured the repre-

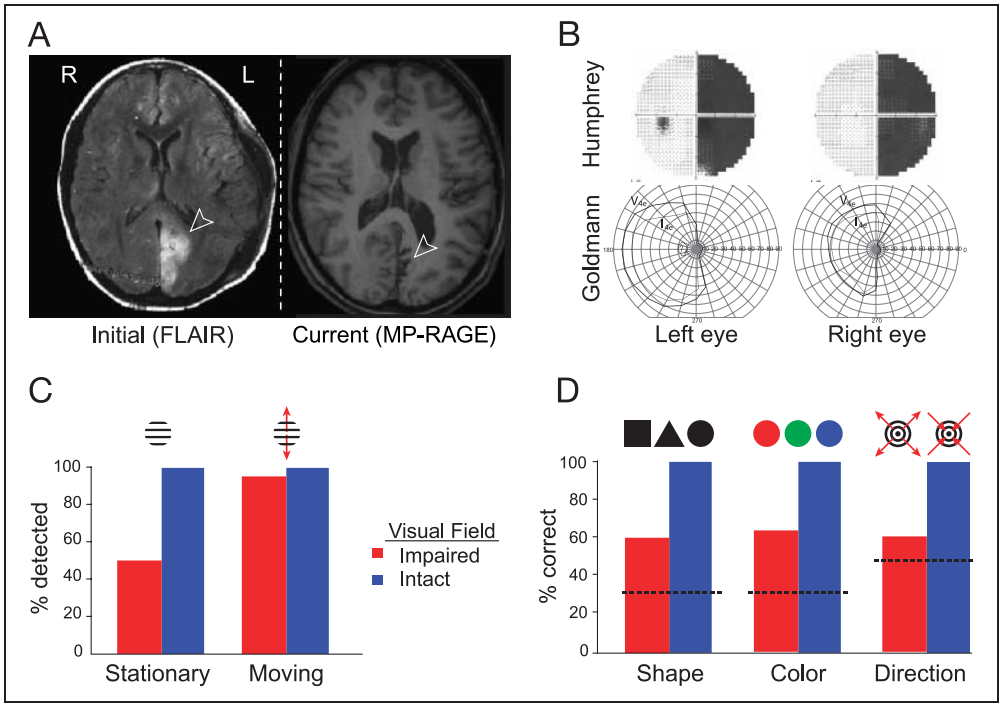

Figure 1. Patient M.C. (A) MRI scans poststroke and 3 years later. Arrows indicate the lesion. (B) Visual fields. Top: Humphrey's automated perimetry 3 months poststroke. Failure to detect a static light stimulus is indicated in black. Bottom: Goldmann's manual perimetry 2 years poststroke. Outline defined by detection of a slowly moving stimulus approaching central fixation. Macular sparing is present. (C) Detection of the onset of moving stimuli was superior as compared to stationary stimuli in the periphery of the affected visual field (χ^2, $p = 2.4 \times 10^{-6}$). (D) Discrimination of shape, color, and direction of motion. Performance was above chance in the impaired visual field (binomial distribution: shape, $p = 1.5 \times 10^{-8}$; color, $p = 1.5 \times 10^{-12}$; motion direction, $p = .007$). Dotted line = chance performance.

sentation of the intact and impaired VFs within striate and extrastriate cortical areas. Visual stimulation of each hemifield was performed separately to allow unambiguous attribution of responses within the damaged hemisphere to the impaired VF. Additionally, we obtained over 3 hours of retinotopic mapping data from M.C. (acquired during multiple scanning sessions) to maximize statistical power, and thus, our ability to detect attenuated neural signals.

The polar angle of visual stimulation was used to define the borders of visual areas by phase reversal (Engel et al., 1994). Within M.C.'s healthy hemisphere, the normal arrangement of visual areas was found (Wandell, Brewer, & Dougherty, 2005) (Figure 2). Within the damaged hemisphere, a retinotopically organized visual cortex was seen, also with the normal arrangement of visual areas including responses from the primary visual cortex. Notably, these responses were found even in the cortex that appears lesioned on structural imaging, including area V1. Examination of cortical responses to varying eccentricity of stimulation (Figure 3) demonstrated that parts of the lesioned cortex responded to stimulation of M.C.'s perimetrically blind field. These responses were present within visual area V1 (Figure 4). Thus, meaningful fMRI responses were obtained from some voxels that contained damaged, but clearly not dead, neural tissue.

Neural and Behavioral Responses to Stimulus Contrast are Attenuated in Blindsight

A puzzle posed by the well-organized retinotopy seen in M.C.'s lesioned hemisphere is the relatively poor quality of her visual perception. If a retinotopically organized cortex (including V1) is present, why is M.C.'s perception of the contralesional hemifield so impaired? We asked if the response properties of the damaged and healthy hemispheres differ, by obtaining neural and psychophysical response functions to moving stimuli over a range of contrast levels. We presented a moving stimulus at the horizontal meridian in the periphery of M.C.'s intact and impaired VF. The stimulus (expanding/contracting concentric rings) was presented at eight different levels of contrast (ranging from 1% to 100%), along with null trials (0% contrast) in a pseudorandomized order. M.C. performed a detection task during behavioral testing and a vigilance task at central fixation during fMRI scanning.

Within M.C.'s healthy hemisphere, cortical responses to peripherally presented, moving stimuli were observed

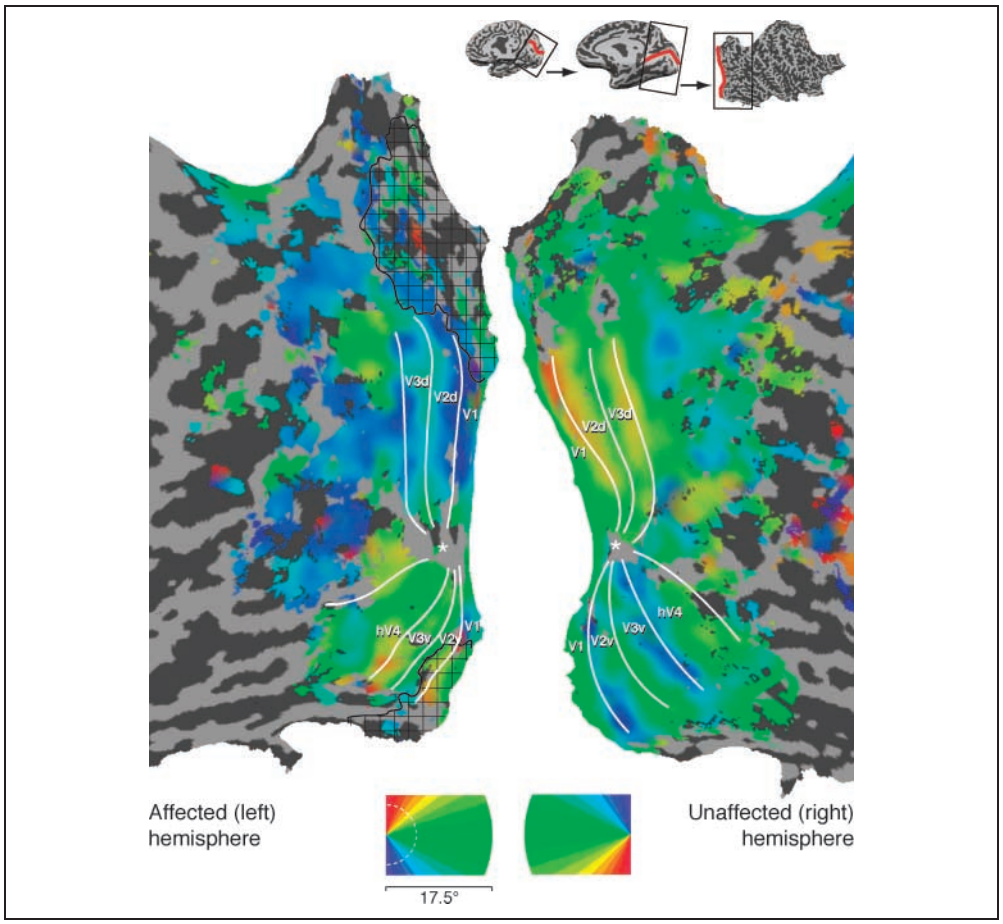

Figure 2. Representation of visual field polar angle. Polar angle representation across the flattened cortical hemispheres, coded by color. The borders of visual areas are indicated by white lines; an asterisk marks the center of the foveal confluence. Gyri are in light and sulci in dark gray; lesion area as defined by anatomical imaging indicated by black hatching. Top inset: Cortical unfolding with the calcarine sulcus in red.

Figure 3. Representation of visual field eccentricity. Eccentricity representation across the flattened cortical hemispheres, coded by color. Labeling conventions are as indicated for Figure 2. Note that "blind" portions of the visual field (>5° eccentricity, indicated by the dotted, white line on the color-coded legend) are represented within area V1 and extrastriate areas.

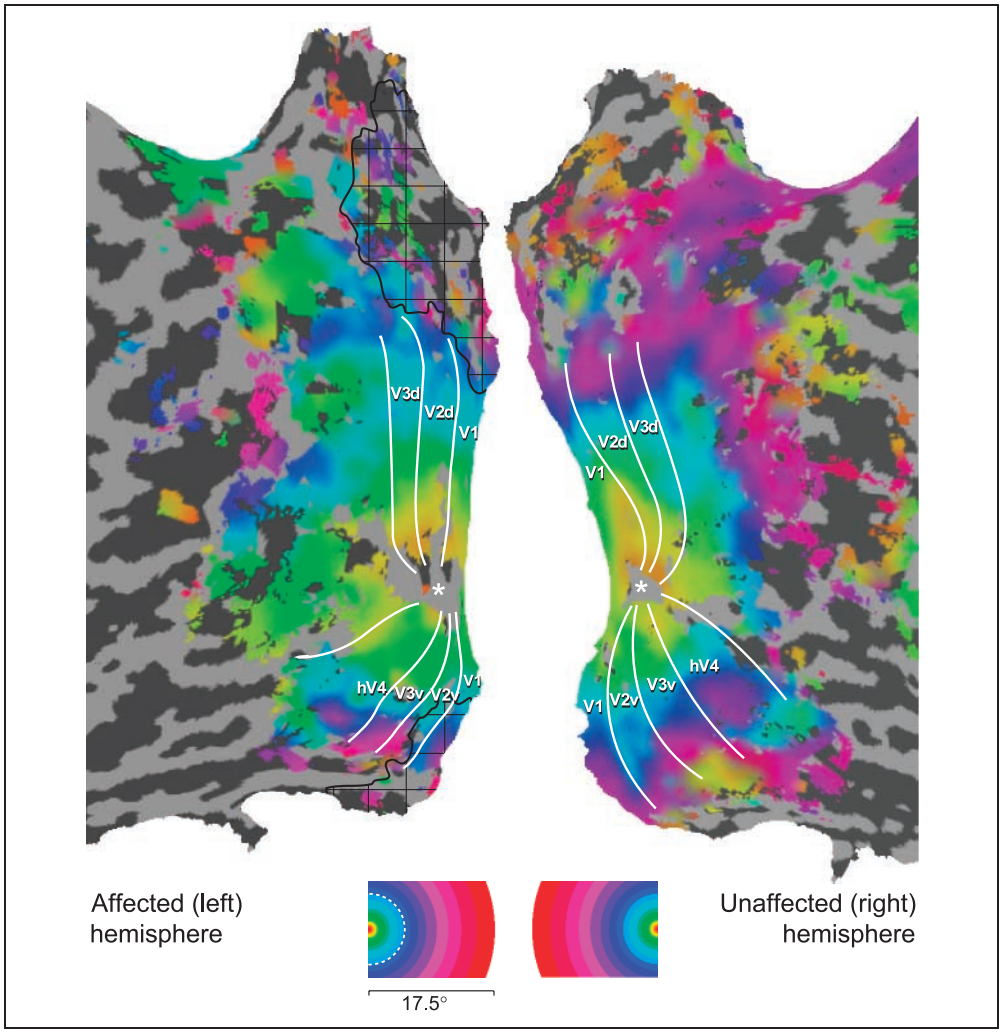

Figure 4. Neuroimaging data from area V1, displayed on inflated but not flattened cortex. The panels present the data from Figures 2, 3, and 5. Label conventions are as specified for those figures.

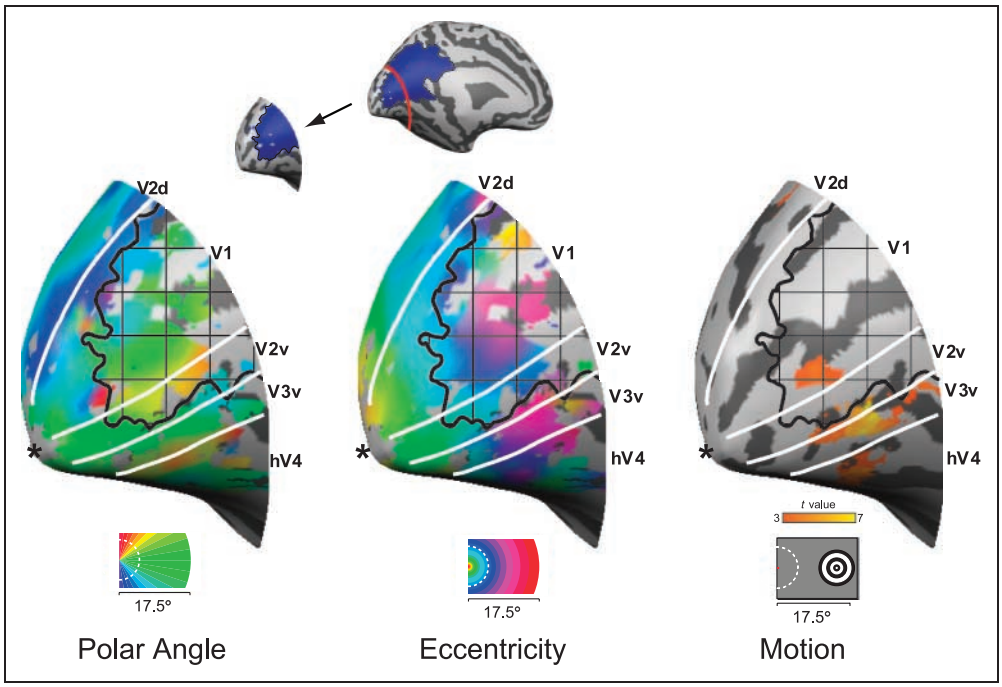

in the motion responsive area (MT), as well as in dorsal and ventral visual areas at the appropriate eccentricity locations (Figure 5A). Within the lesioned hemisphere, responses were confined to MT, ventral V1, V2/V3, and the portion of hV4 representing the upper visual quadrant. Notably, the activation occurred at the appropriate eccentricities in the damaged hemisphere as suggested by retinotopic mapping (compare Figures 3 and 5A), supporting our observation of a retinotopically organized cortex representing M.C.'s perimetrically blind VF. Again, the V1 response to visual stimulation of the blind hemifield was located within the cortex that appeared lesioned on structural imaging. This is more clearly demonstrated in Figure 4, which identifies the

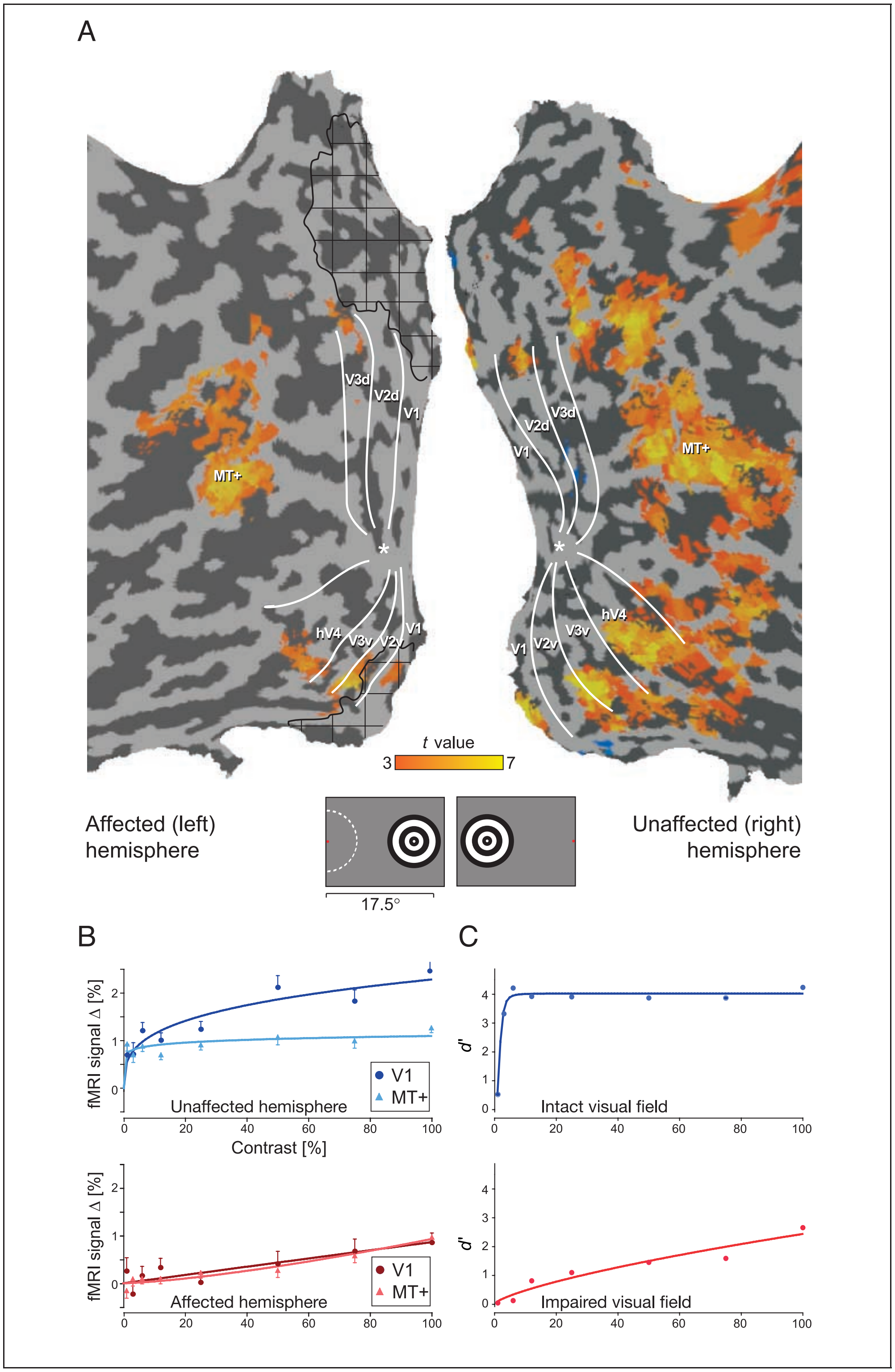

Figure 5. Effect of stimulus contrast upon neural response and perceptual performance. (A) Response to the 100% contrast stimulus (mapwise cluster-corrected $p < .03$ within posterior visual areas). M.C. monitored a fixation point (red dot on the legend), while expanding and contracting concentric rings were presented in the visual periphery at varying contrast levels. The extent of M.C.'s macular sparing is indicated by the dashed, white line. Note that the position of activity seen here corresponds to the expected eccentricity locations shown in Figure 3. (B) Neural contrast response functions in area V1 and MT for the unaffected and affected hemispheres (±*SEM*). (C) M.C.'s psychophysical detection performance over a range of contrast levels, expressed as d'.

responsive voxels within area V1 in relation to the lesioned cortex.

To determine the relationship between neural response and contrast, we obtained the average fMRI signal change for each contrast level in each visual area (Figure 5B; responses from additional visual areas are presented in the Supplementary Figure). Within the healthy hemisphere, the contrast-response functions were comparable to those seen in previous studies of normal control subjects (Liu & Wandell, 2005): Area MT showed little sensitivity to changes in contrast level, whereas V1 responses were modulated over a two- to three-fold range. The contrast-response functions measured in the lesioned hemisphere, however, were markedly attenuated with a greater dependence upon contrast level. Of note, the maximal fMRI signal change observed within the lesioned V1 cortex was approximately one-third that seen in the intact hemisphere.

How were these attenuated neural responses related to M.C.'s visual performance? We evaluated M.C.'s ability to detect the stimuli across a range of contrast levels (Figure 5C). Although performance in the unaffected VF was nearly perfect for all but the lowest contrast level, detection performance within the impaired VF was markedly diminished, with a psychometric function that was far more dependent upon contrast than seen in the intact VF. The perceptual performance within the intact and impaired VFs mirrored the neural response functions obtained from the lesioned and healthy hemispheres, respectively.

Responses from Lesioned Cortex

To further evaluate the position of cortical responses to visual stimulation in the damaged hemisphere, we obtained high-resolution, T2-weighted structural images through M.C.'s occipital lobe. Figure 6 presents the location of voxels that were significantly activated by moving stimuli presented in the nominally blind field. As can be seen, responses were present within the lesioned and atrophic cortex, including a remnant of the inferior bank of the calcarine sulcus, corresponding both anatomically and on retinotopic mapping to area V1.

DISCUSSION

Patient M.C. is Phenomenologically Similar to Other Blindsight Cases

Cases of clinical blindsight are fairly infrequent. As a consequence, the few patients with residual visual abilities after V1 lesion have been studied intensively. Our patient, M.C., is similar in many respects to these prior cases. Patient G.Y., for example, had a striate lesion after traumatic brain injury at a young age (8 years old), resulting in a perimetric hemianopia with macular sparing. Within his impaired field, he demonstrates a statokinetic dissociation (Sahraie et al., 1997) and an above-chance discrimination of color, shape, and direction of motion (Benson, Guo, & Blakemore, 1998). G.Y. has some conscious awareness for visual stimuli (Stoerig & Barth, 2001), although he denies ''seeing'' objects and reports ''guessing'' in forced-choice paradigms. Like M.C., Patient G.Y.'s perceptual abilities correlate with stimulus contrast (Stoerig, Zontanou, & Cowey, 2002). Other patients with lesions in the occipital cortex have exhibited above-chance discrimination of motion direction (Schoenfeld et al., 2002; Perenin, 1991) and shape (Marcel, 1998; Stoerig & Cowey, 1997), and some degree of conscious awareness of stimulation in the affected

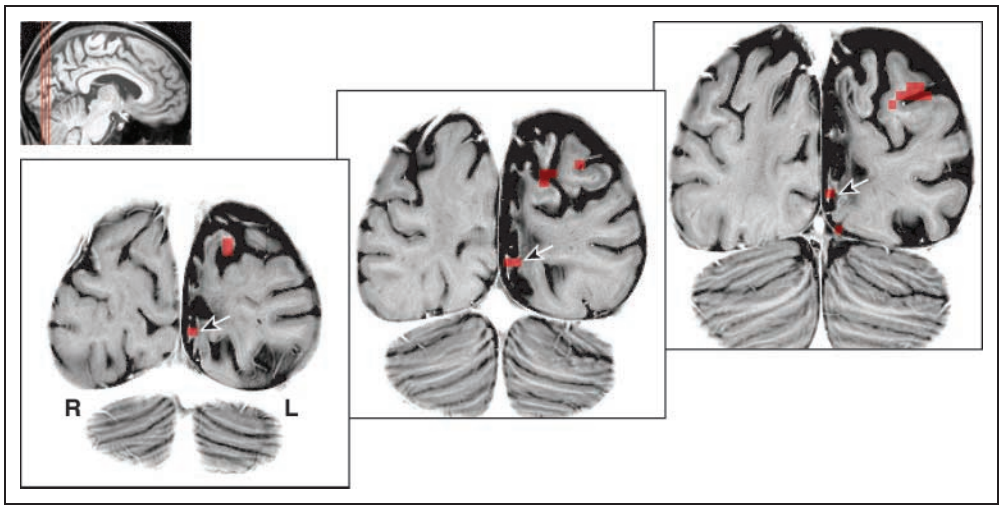

Figure 6. Cortical responses to moving stimuli displayed on a high-resolution anatomical scan. The areas of significant cortical response to peripheral stimulation of the impaired visual field (Figure 5A) are displayed atop high-resolution, coronal T2-weighted images. The location of the area V1 response (as determined by retinotopic mapping) is indicated (arrows). The lesioned cortex is atrophied with altered white matter signal. The indicated area of activation is on the lower bank of the calcarine sulcus, which itself is distorted and enlarged from the surrounding loss of cerebral volume. (Structural image gray scale inverted for ease of viewing).

field. Therefore, M.C. is characteristic of other patients with the neuropsychological phenomenon of blindsight.

V1 Activity in Blindsight

Studies of residual vision in monkeys with V1 lesions (Weiskrantz et al., 1977) have shown that subcortical pathways to extrastriate areas can support visual function. There is also evidence, however, that patients can have residual vision in small portions of the blind VF, suggesting that spared ''islands'' of the V1 cortex mediate vision in some cases of blindsight (Wessinger et al., 1999; Fendrich et al., 1992). Additionally, moving or pattern-reversal stimuli presented to the affected VF elicited striate cortex responses in two out of four blindsight patients (Morland et al., 2004; Kleiser et al., 2001). Therefore, there is the intriguing possibility that what appears to be the same behavioral phenotype (low confidence but accurate detection of moving stimuli in a perimetrically blind field) may be mediated by different neural mechanisms in different patients.

In our current study, we not only confirmed that responses in the early visual cortex (including V1) can accompany the behavioral signature of blindsight performance but also described the properties and organization of these visual areas. Within the cortex that appears lesioned on anatomical imaging, we identified responses from area V1 that are retinotopically organized to represent M.C.'s perimetrically blind field and manifest an attenuated contrast-response function that mirrors her psychometric performance.

Although responses from the damaged cortex might be dismissed initially as artifact or the consequence of altered neurovascular coupling following ischemia and stroke (Roc et al., 2006; Marshall, 2004), several features of the response we observed demonstrate its functional significance. The location of activity produced by presentation of a moving stimulus was concordant with assigned eccentricity calculated by retinotopic mapping. Moreover, the response of this region was appropriately modulated by stimulus contrast. Just as a patient need not only be normally ''sighted'' or ''blind,'' a continuum of cortical damage following ischemic injury exists (Mitsias et al., 2004). In the case of M.C., the cortex in the area of her stroke was atrophied and gliotic, leaving the possibility of residual function. In other cases, damage results in a cystic region in which no neurons may be reasonably expected to remain. Patients with blindsight vary in this regard as well (Stoerig et al., 2002).

Could poor control of eye movements explain our findings? During initial behavioral testing, eye movements were tracked and M.C. demonstrated excellent cooperation with central fixation. During scanning, M.C. performed a constant vigilance task at central fixation. Her performance was generally high, and scanning periods during which performance was lower were excluded from the contrast-response analysis. It is, nonetheless, possible that M.C. made covert eye movements during testing. Eye movements may be responsible for better performance on behavioral testing, although the altered shape of her psychometric contrast-response function would be difficult to explain on this basis. Additionally, a tendency to directly view the retinotopic mapping stimuli during scanning would not be expected to alter the shape of the observed map, but instead create areas of nonresponsive cortex (as the stimulus would be now stimulating the foveal confluence). Thus, although imperfect control of eye movements may have contributed to an inflation of measured behavioral performance, they cannot easily explain our neuroimaging findings.

A Functional Role for V1 and MT

In our study, we measured both M.C.'s behavioral and neural contrast-response functions. We found that the observed responses in areas V1 and MT are modulated by stimulus contrast in both hemispheres, although the shapes of these responses in the affected hemisphere are altered relative to the intact hemisphere, and reflect M.C.'s impaired psychometric performance.

What may we conclude regarding the functional role of these visual areas in her spared vision? Although the correspondence between her perceptual performance and the neural responses within V1 might be taken initially as evidence that V1 is necessary for her spared vision, this is not required to be the case. It remains possible that M.C.'s vision within the blind field is supported by direct projections from subcortical areas. The neural contrast sensitivity plots (Figure 5B) reveal that the MT responses in the two hemispheres are very similar in magnitude for 100% stimulus contrast, whereas the V1 response in the affected hemisphere is one-third that observed in the unaffected hemisphere. It may be the case that, at the highest contrast level, input from subcortical pathways to MT (despite or in addition to an attenuated V1 input) is sufficient to generate close-to-normal levels of MT activation. For lower contrast stimuli, the signal from V1 may predominate. The idea that cortical and subcortical projections differ in the range of transmitted contrast information is supported by findings in a macaque with complete ablation of V1 showing that residual vision is preserved for high- rather than low-contrast stimuli (Stoerig et al., 2002).

Furthermore, we might consider the extreme case that the observed V1 activity is driven entirely in a top–down manner from MT. The contrast-response functions of V1 and MT within the affected hemisphere (Figure 5B) are similar in shape and amplitude. In addition, top–down modulation of early visual areas by MT has been observed by magnetoencephalography in another blindsight patient (Schoenfeld et al., 2002). Techniques with higher temporal resolution (such as magnetoencephalography and/or ERP) would be required to explore whether the peak activation within V1 occurs prior to or after

the peak activation within MT, and could be the focus of further studies with Patient M.C. There are, however, limits to the extent to which responses in V1 might be explained by top–down input. For example, it would be difficult to explain the presence of well-organized retinotopic maps in early visual areas (V1, V2, V3) of the affected hemisphere, given the relatively coarse retinotopic organization observed in area MT (Van Essen, Maunsell, & Bixby, 1981, however, see Huk, Dougherty, & Heeger, 2002).

In our study, it was necessary to combine data from several sessions, acquired at high field strength and with surface coil techniques, to reliably identify responses from the striate cortex. Given that the magnitude of maximal response in the lesioned V1 was one-third that of the intact hemisphere, we might have failed to identify this activation if less data had been acquired. Notably, the attenuation of neural response in M.C.'s damaged hemisphere was much greater in striate than in extrastriate areas. It is therefore possible that an imaging study with less data might detect extrastriate responses but fail to resolve a weak striate signal.

In summary, we have demonstrated the presence of retinotopically organized, functionally responsive V1 cortex representing the nominally blind field of a patient with blindsight. Attenuated neural contrast-response functions were found to correlate with M.C.'s impaired psychophysical performance. These results demonstrate that graded performance is associated with graded neural responses in V1, even in the absence of conscious visual perception.

Acknowledgments

We thank Patient M.C. for her patience and cooperation, Dr. Grant Liu for his clinical insights, and Dr. Anjan Chatterjee for his guidance in our initial studies. G. K. A. is supported by a Burroughs-Wellcome Career Development Award. D. H. B. is supported by NEI EY10016. Support was also provided by NEI P30 EY001583.

Reprint requests should be sent to Geoffrey K. Aguirre, Department of Neurology, Hospital of the University of Pennsylvania, 3400 Spruce Street, Philadelphia, PA 19104, or via e-mail: aguirreg@mail.med.upenn.edu.

REFERENCES

Aguirre, G. K., Zarahn, E., & D'Esposito, M. (1998). The variability of human, bold hemodynamic responses. *Neuroimage, 8,* 360–369.

Baseler, H. A., Morland, A. B., & Wandell, B. A. (1999). Topographic organization of human visual areas in the absence of input from primary cortex. *Journal of Neuroscience, 19,* 2619–2627.

Benson, P. J., Guo, K., & Blakemore, C. (1998). Direction discrimination of moving gratings and plaids and coherence in dot displays without primary visual cortex (V1). *European Journal of Neuroscience, 10,* 3767–3772.

Blythe, I. M., Bromley, J. M., Kennard, C., & Ruddock, K. H. (1986). Visual discrimination of target displacement remains after damage to the striate cortex in humans. *Nature, 320,* 619–621.

Bruce, C. J., Desimone, R., & Gross, C. G. (1986). Both striate cortex and superior colliculus contribute to visual properties of neurons in superior temporal polysensory area of macaque monkey. *Journal of Neurophysiology, 55,* 1057–1075.

Cao, J. (1999). The size of the connected components of excursion sets of χ^2, t and f fields. *Advances in Applied Probability, 31,* 579–595.

Cowey, A. (2004). The 30th Sir Frederick Bartlett lecture: Fact, artefact, and myth about blindsight. *Quarterly Journal of Experimental Psychology, Section A: Human Experimental Psychology, 57,* 577–609.

Engel, S. A., Glover, G. H., & Wandell, B. A. (1997). Retinotopic organization in human visual cortex and the spatial precision of functional MRI. *Cerebral Cortex, 7,* 181–192.

Engel, S. A., Rumelhart, D. E., Wandell, B. A., Lee, A. T., Glover, G. H., Chichilnisky, E. J., et al. (1994). fMRI of human visual cortex. *Nature, 369,* 525.

Fendrich, R., Wessinger, C. M., & Gazzaniga, M. S. (1992). Residual vision in a scotoma: Implications for blindsight. *Science, 258,* 1489–1491.

Fendrich, R., Wessinger, C. M., & Gazzaniga, M. S. (2001). Speculations on the neural basis of islands of blindsight. *Progress in Brain Research, 134,* 353–366.

Goebel, R., Muckli, L., Zanella, F. E., Singer, W., & Stoerig, P. (2001). Sustained extrastriate cortical activation without visual awareness revealed by fMRI studies of hemianopic patients. *Vision Research, 41,* 1459–1474.

Huk, A. C., Dougherty, R. F., & Heeger, D. J. (2002). Retinotopy and functional subdivision of human areas MT and MST. *Journal of Neuroscience, 22,* 7195–7205.

Kasten, E., Wuest, S., & Sabel, B. A. (1998). Residual vision in transition zones in patients with cerebral blindness. *Journal of Clinical and Experimental Neuropsychology, 20,* 581–598.

Kiebel, S. J., Poline, J. B., Friston, K. J., Holmes, A. P., & Worsley, K. J. (1999). Robust smoothness estimation in statistical parametric maps using standardized residuals from the general linear model. *Neuroimage, 10,* 756–766.

Kleiser, R., Wittsack, J., Niedeggen, M., Goebel, R., & Stoerig, P. (2001). Is V1 necessary for conscious vision in areas of relative cortical blindness? *Neuroimage, 13,* 654–661.

Liu, J., & Wandell, B. A. (2005). Specializations for chromatic and temporal signals in human visual cortex. *Journal of Neuroscience, 25,* 3459–3468.

Marcel, A. J. (1998). Blindsight and shape perception: Deficit of visual consciousness or of visual function? *Brain, 121,* 1565–1588.

Marshall, R. S. (2004). The functional relevance of cerebral hemodynamics: Why blood flow matters to the injured and recovering brain. *Current Opinion in Neurology, 17,* 705–709.

Mitsias, P. D., Ewing, J. R., Lu, M., Khalighi, M. M., Pasnoor, M., Ebadian, H. B., et al. (2004). Multiparametric iterative self-organizing MR imaging data analysis technique for assessment of tissue viability in acute cerebral ischemia. *AJNR, American Journal of Neuroradiology, 25,* 1499–1508.

Morland, A. B., Jones, S. R., Finlay, A. L., Deyzac, E., Le, S., & Kemp, S. (1999). Visual perception of motion, luminance and colour in a human hemianope. *Brain, 122,* 1183–1198.

Morland, A. B., Le, S., Carroll, E., Hoffmann, M. B., & Pambakian, A. (2004). The role of spared calcarine cortex and lateral occipital cortex in the responses of human hemianopes to visual motion. *Journal of Cognitive Neuroscience, 16,* 204–218.

Morris, J. S., DeGelder, B., Weiskrantz, L., & Dolan, R. J. (2001). Differential extrageniculostriate and amygdala responses to presentation of emotional faces in a cortically blind field. *Brain, 124,* 1241–1252.

Naka, K. I., & Rushton, W. A. (1966). S-potentials from colour units in the retina of fish (Cyprinidae). *Journal of Physiology, 185,* 536–555.

Perenin, M. T. (1991). Discrimination of motion direction in perimetrically blind fields. *NeuroReport, 2,* 397–400.

Poppel, E., Held, R., & Frost, D. (1973). Residual visual function after brain wounds involving the central visual pathways in man. *Nature, 243,* 295–296.

Riddoch, G. (1917). Dissociation of visual perceptions due to occipital injuries, with especial reference to appreciation of movement. *Brain: A Journal of Neurology, 40,* 15–57.

Roc, A. C., Wang, J., Ances, B. M., Liebeskind, D. S., Kasner, S. E., & Detre, J. A. (2006). Altered hemodynamics and regional cerebral blood flow in patients with hemodynamically significant stenoses. *Stroke, 37,* 382–387.

Rodman, H. R., Gross, C. G., & Albright, T. D. (1989). Afferent basis of visual response properties in area MT of the macaque: I. Effects of striate cortex removal. *Journal of Neuroscience, 9,* 2033–2050.

Rodman, H. R., Gross, C. G., & Albright, T. D. (1990). Afferent basis of visual response properties in area MT of the macaque: II. Effects of superior colliculus removal. *Journal of Neuroscience, 10,* 1154–1164.

Sahraie, A., Weiskrantz, L., Barbur, J. L., Simmons, A., Williams, S. C., & Brammer, M. J. (1997). Pattern of neuronal activity associated with conscious and unconscious processing of visual signals. *Proceedings of the National Academy of Sciences, U.S.A., 94,* 9406–9411.

Scharli, H., Harman, A. M., & Hogben, J. H. (1999a). Blindsight in subjects with homonymous visual field defects. *Journal of Cognitive Neuroscience, 11,* 52–66.

Scharli, H., Harman, A. M., & Hogben, J. H. (1999b). Residual vision in a subject with damaged visual cortex. *Journal of Cognitive Neuroscience, 11,* 502–510.

Schoenfeld, M. A., Noesselt, T., Poggel, D., Tempelmann, C., Hopf, J. M., Woldorff, M. G., et al. (2002). Analysis of pathways mediating preserved vision after striate cortex lesions. *Annals of Neurology, 52,* 814–824.

Sereno, M. I., McDonald, C. T., & Allman, J. M. (1994). Analysis of retinotopic maps in extrastriate cortex. *Cerebral Cortex, 4,* 601–620.

Standage, G. P., & Benevento, L. A. (1983). The organization of connections between the pulvinar and visual area MT in the macaque monkey. *Brain Research, 262,* 288–294.

Stoerig, P., & Barth, E. (2001). Low-level phenomenal vision despite unilateral destruction of primary visual cortex. *Consciousness and Cognition, 10,* 574–587.

Stoerig, P., & Cowey, A. (1997). Blindsight in man and monkey. *Brain, 120,* 535–559.

Stoerig, P., & Cowey, A. (2007). Blindsight. *Current Biology, 17,* R822–R824.

Stoerig, P., Zontanou, A. H., & Cowey, A. (2002). Aware or unaware: Assessment of cortical blindness in four men and a monkey. *Cerebral Cortex, 12,* 565–574.

Tomaiuolo, F., Ptito, M., Marzi, C. A., Paus, T., & Ptito, A. (1997). Blindsight in hemispherectomized patients as revealed by spatial summation across the vertical meridian. *Brain, 120,* 795–803.

Tong, F. (2003). Primary visual cortex and visual awareness. *Nature Reviews Neuroscience, 4,* 219–229.

Van Essen, D. C., Maunsell, J. H., & Bixby, J. L. (1981). The middle temporal visual area in the macaque: Myeloarchitecture, connections, functional properties, and topographic organization. *Journal of Comparative Neurology, 199,* 293–326.

Wandell, B. A., Brewer, A. A., & Dougherty, R. F. (2005). Visual field map clusters in human cortex. *Philosophical Transactions of the Royal Society of London, Series B, Biological Sciences, 360,* 693–707.

Weiskrantz, L. (1996). Blindsight revisited. *Current Opinion in Neurobiology, 6,* 215–220.

Weiskrantz, L., Cowey, A., & Passingham, C. (1977). Spatial responses to brief stimuli by monkeys with striate cortex ablations. *Brain, 100,* 655–670.

Weiskrantz, L., Warrington, E. K., Sanders, M. D., & Marshall, J. (1974). Visual capacity in the hemianopic field following a restricted occipital ablation. *Brain, 97,* 709–728.

Wessinger, C. M., Fendrich, R., & Gazzaniga, M. S. (1997). Islands of residual vision in hemianopic patients. *Journal of Cognitive Neuroscience, 9,* 203–221.

Wessinger, C. M., Fendrich, R., & Gazzaniga, M. S. (1999). Variability of residual vision in hemianopic subjects. *Restorative Neurology and Neuroscience, 15,* 243–253.

Worsley, K. J., & Friston, K. J. (1995). Analysis of fMRI time-series revisited—Again. *Neuroimage, 2,* 173–182.

Worsley, K. J., Marrett, S., Neelin, P., Vandal, A. C., Friston, K. J., & Evans, A. C. (1996). A unified statistical approach for determining significant signals in images of cerebral activation. *Human Brain Mapping, 4,* 58–73.

Zarahn, E., Aguirre, G. K., & D'Esposito, M. (1997). Empirical analyses of bold fMRI statistics: I. Spatially unsmoothed data collected under null-hypothesis conditions. *Neuroimage, 5,* 179–197.

Zeki, S., & Ffytche, D. H. (1998). The Riddoch syndrome: Insights into the neurobiology of conscious vision. *Brain, 121,* 25–45.